coatings

MDPI

Article

Synergistic Effect of Addition of Fillers on Properties of Interior Waterborne UV-Curing Wood Coatings

Xiaoxing Yan [1], Xingyu Qian [1], Rong Lu [2,*] and Tetsuo Miyakoshi [2]

[1] College of Furnishings and Industrial Design, Nanjing Forestry University, Nanjing 210037, China; yanxiaoxing@njfu.edu.cn (X.Y.); qianxingyu@njfu.edu.cn (X.Q.)

[2] Department of Industrial Chemistry, School of Science and Technology, Meiji University, Kawasaki-shi 214-8571, Japan; miya@meiji.ac.jp

* Correspondence: lurong@meiji.ac.jp; Tel./Fax: +81-44-9347784

Received: 9 November 2017; Accepted: 20 December 2017; Published: 23 December 2017

Abstract: A waterborne ultraviolet (UV)-curing coating was prepared on the surface of wood materials with modification of talcum powder and calcium carbonate ($CaCO_3$). When the waterborne UV-curing coatings on the surface of wood materials (WUVCW) was radiated for 1 min by UV (λ = 365 nm) and dried at 40 °C for 10 min, it showed good hardness, adhesion, and impact strength, with controlling the talcum content of 2.0% and $CaCO_3$ content of 1.0%, respectively. When the content of talcum powder was higher than 2%, the mechanical properties and gloss of the WUVCW decreased, and when the talcum powder of WUVCW increase to more than 5%, a matte surface appeared after curing. When $CaCO_3$ and talcum powder were present at the same time, the mechanical properties of WUVCW were better than those of only $CaCO_3$ or talcum powder.

Keywords: modification; interior waterborne coating; UV; mechanical properties; gloss

1. Introduction

Wood coatings can play a decorative and protective role on carpentry and woodwork [1]. Ultraviolet (UV) curing coatings can be rapidly solidified under the irradiation of UV, and the main components of the coating are light initiator, reactive oligomer, and active thinner [2]. UV curing is environmentally friendly and more efficient when compared to the traditional wood coatings [3]. UV curing coatings with high solid content are also used in industry—solidification by UV only few seconds. However, the active thinner, such as acrylic functional monomer, has the volatility, which will produce bad materials harm to the human health [4]. Waterborne coating uses water as thinner and contains a small amount of organic solvent. It not only can reduce the cost of the coating, but also significantly reduce the emission of volatile organic compounds (VOC) [5]. Waterborne coating is becoming more and more favorable for environment, such as non-toxic, no odor, not burning, high safety, and so on [6]. But the evaporation of water needs a lot of heat energy, and the cure rate of the waterborne coating is slow [7]. Waterborne UV-curing coatings on the wood materials (WUVCW) combine the advantages of UV curing and waterborne coating, which not only eliminates the pollution caused by VOC, but it also has the characteristics of rapid solidification and energy saving [8].

At present, the water soluble photosensitive resin is the most important component in UV-curing coating material and it mainly includes unsaturated polyester, polyurethane acrylate (PUA), polyacrylate, and polyester acrylate [9]. By comparison, the preparation of WUVCW by the PUA resin as the pre-polymerization system has been reported [10]. Gloss is an important indicator of the optical properties of the coating [11]. Very high gloss may even cause some damage to eyesight, and the low gloss attracts more and more people in the field of wood coating. To achieve the control of gloss is an important part of a successful coating [12]. However, WUVCW usually showed a poor mechanical property and high gloss that strongly affects its application in wood surface [13]. Therefore,

it is necessary to modify the WUVCW in order to improve the mechanical properties and reduce the gloss [14].

Wu et al. [15] used the antimony doped tin oxide to UV curable waterborne poly(urethane-acrylate) for the modification of thermal insulation by sol-gel process. Liao et al. [16] used carbon nitride to reinforce the mechanical and thermal properties of UV-curable waterborne polyurethane acrylate coatings. Rahman et al. [17] studied nanoferrite on the anticorrosive property of waterborne epoxy-acrylate coatings. Lv et al. [18] used silica on the thermochromics property of waterborne UV-curable polyurethane acrylate nanocomposites coatings. Talcum powder has an advantage of low price, stability of the physical and chemical properties, tasteless, and non-toxic [19]. The particles have the typical scaly, which can improve the heat resistance and bending resistance of the material. Talcum appears inert in most chemical reagents, and does not break down when contacted with acid [20]. Talcum has the low thermal conductivity and high thermal shock resistance, and still not decomposed when heated to 900 °C [21]. The excellent properties of talcum powder make it the good filler and can be used as an additive for coatings. Calcium carbonate ($CaCO_3$) is the white powder that is non-toxic, tasteless, none irritating, cheap and rich in resources, and has been widely used in plastic and ink fields [22].

The manuscript presented an interesting research on the optimization of the wood coatings by modifying the coating's composition in order to maximize the output quality. Used coating components are somewhat more environmentally friendly than the ones that are commonly used. In this paper, talcum powder and $CaCO_3$ were combined to modify the WUVCW, and compared with single use of $CaCO_3$ or talcum. Heating with UV curing is used in combination during this technology. The orthogonal experiment was used to select and optimize the parameters of synergistic effect of talcum and $CaCO_3$. The purpose of the synergistic modification is to enhance the mechanical properties and to reduce the gloss of the WUVCW.

2. Experimental

2.1. Materials

All of the reagents in the experiment were pure without further processing. The substrates were supplied by Yihua Lifestyle Technology Co. Ltd., Shantou, China. The base substrates were Eucalyptus and Poplar composite wood, the middle part was provided with 3 layers of poplar veneer, and 2 pieces of Eucalyptus veneers were symmetrically placed on both sides of the Poplar. Isophorone diisocyanate (IPDI, M_w: 222.28 g/mol, CAS No.: 4098-71-9), polyether diol (PED, M_w: 2000 g/mol, CAS No.: 25322-69-4), 2,2-dimethylol propionic acid (DPA, M_w: 134.13 g/mol, CAS No.: 4767-03-7), hydroxyethyl methacrylate (HM, M_w: 130.14 g/mol, CAS No.: 868-77-9), tripropylene glycol diacrylate (TGD, M_w: 300.35 g/mol, CAS No.: 42978-66-5), and light initiator 2,4,6-trimethyl benzoyl diphenyl phosphine oxide (TBDPO, M_w: 348.4 g/mol, CAS No.: 75980-60-8) were purchased from Daguangming Chemical Reagent Nanjing Co., Ltd., Nanjing, China. IPDI, PED and HM were used as resin. DPA was used as chain extender. TGD was used as reactive thinner. TBDPO was used as photoinitiator. Fillers $CaCO_3$, and talcum were provided by Shanghai Chemical Reagent Co., Ltd. (Shanghai, China) and the specification is 99.5%, 200 nm + 30 nm, Aladdin reagents. The commercial waterborne UV-curing coatings were supplied by Guangdong Huarun Paint Chemical Co., Ltd., Foshan, China.

2.2. Preparation of Coating

The substrates (100 mm × 100 mm × 5 mm) were pretreated, and polished with sandpaper. The roughness of wooden substrate was about 3 μm. The grit of used sandpaper was 1000. Firstly, the pre-weighed IPDI, HM, DPA, TGD, and TBDPO were mixed with the PED to put into the four-necked flasks with condenser tube, agitator, and thermometer to obtain the waterborne UV-curing coatings. The rotation speed was 100 rpm. The system reacted at 75 °C for 4 h, and then the temperature dropped slowly to the room temperature. Waterborne UV-curing coatings comprise the following components:

the content of IPDI was 35.0%, the content of PED was 15.2%, the content of DPA was 5.8%, the content of HM was 30.0%, the content of TGD was 10.0%, and the content of TBDPO was 4.0%. The pH value of the obtained waterborne UV-curing coatings was about 7.0, and the solid content was about 26.5%. The pre-designed amount of $CaCO_3$ and talcum were added to the waterborne UV-curing coatings (control the content of $CaCO_3$ and talcum in WUVCW was 1.0%–6.0%), stirring evenly, and then the system was stirred at room temperature for 1 h. The formulations are summarized in Table 1. The coating was sprayed on the substrate prior to the primer treatment by a fast rotating motor and a certain pressure jet (98PSI, ANEST IWATA Corporation, Yokohama, Japan). The resulting coating was placed in an oven at 40 °C for 10 min, and was then solidified under UV radiation of the middle pressure mercury lamp (400 W) at 365 nm. The dry curing time (1.0–3.0 min) was controlled in the radiation curing. The coating was gently grinded with 1000 grit of sandpaper and the dust was wiped off with a dry cloth. The spray step was repeated for three times. The coating thickness was about 60 μm. The deviation of the coating thickness was 0.01 μm. UV radiation time of sample 2 and 3 was 3.0 min, and UV radiation time of other samples was 1.0 min. The thickness of the coating has no influence on the UV curing time in a certain range. Only when the coating thickness is greater than 300 μm, the curing time will increase slightly. The commercial waterborne UV-curing coatings without $CaCO_3$ and talcum were prepared according to the same process and the coating thickness was about 60 μm for comparison.

Table 1. Composition of waterborne UV-curing coatings on the wood materials (WUVCW).

Sample	IPDI (g)	PED (g)	DPA (g)	HM (g)	TGD (g)	TBDPO (g)	$CaCO_3$ (g)	Talcum (g)	UV Radiation Time (min)
1	34.3	14.9	5.7	29.4	9.8	3.9	1.0	1.0	1.0
2	32.9	14.3	5.5	28.2	9.4	3.8	1.0	5.0	3.0
3	32.9	14.3	5.5	28.2	9.4	3.8	5.0	1.0	3.0
4	31.5	13.7	5.2	27.0	9.0	3.6	5.0	5.0	1.0
5	34.7	15.0	5.7	29.7	9.9	4.0	1.0	0	1.0
6	34.0	14.7	5.6	29.1	9.7	3.9	1.0	2.0	1.0
7	33.6	14.6	5.6	28.8	9.6	3.8	1.0	3.0	1.0
8	33.3	14.4	5.5	28.5	9.5	3.8	1.0	4.0	1.0
9	32.9	14.3	5.5	28.2	9.4	3.8	1.0	5.0	1.0
10	32.6	14.1	5.4	27.9	9.3	3.7	1.0	6.0	1.0
11	35.0	15.2	5.8	30.0	10.0	4.0	0	0	1.0
12	34.8	15.1	5.8	29.9	10.0	4.0	0	0.5	1.0
13	34.7	15.0	5.7	29.7	9.9	4.0	0	1.0	1.0
14	34.3	14.9	5.7	29.4	9.8	3.9	0	2.0	1.0
15	34.0	14.7	5.6	29.1	9.7	3.9	0	3.0	1.0
16	33.6	14.6	5.6	28.8	9.6	3.8	0	4.0	1.0
17	33.3	14.4	5.5	28.5	9.5	3.8	0	5.0	1.0
18	32.9	14.3	5.5	28.2	9.4	3.8	0	6.0	1.0
19	34.8	15.1	5.8	29.9	10.0	4.0	0.5	0	1.0
20	34.3	14.9	5.7	29.4	9.8	3.9	2.0	0	1.0
21	34.0	14.7	5.6	29.1	9.7	3.9	3.0	0	1.0
22	33.6	14.6	5.6	28.8	9.6	3.8	4.0	0	1.0
23	33.3	14.4	5.5	28.5	9.5	3.8	5.0	0	1.0
24	32.9	14.3	5.5	28.2	9.4	3.8	6.0	0	1.0

In this experiment, the main factors that affect the modification of WUVCW were talcum content, $CaCO_3$ content, and UV radiation time [9]. Full factorial experiment design is that all combinations of all levels for all the factors are carried out at least one experiment, and the required number of experiments is the most, therefore, the cost of material and time is also the most. When these three factors are optimized through orthogonal experiment, the mechanical properties of the modified coatings can be optimized after synergistic modification. Orthogonal experiment was used to optimize the effect of three factors on the synergistic modification. The principle of orthogonal experiment is based on statistical principle and orthogonal theory. It is a mathematical method of multi factor experiment, which can deal with some complex problems more conveniently. Three factors and two levels orthogonal experiments were designed, and there were four experiments (samples 1–4 in Table 1)

in the orthogonal experiment (Table 2). Factor A is the content of $CaCO_3$ in the range of 1.0%–5.0%. Factor B is the content of talcum in the range of 1.0%–5.0%. Factor C is the UV radiation time in the range of 1.0–3.0 min. Two levels of $CaCO_3$ content were 1.0% and 5.0%, respectively. Two levels of talcum content were 1.0% and 5.0%, respectively. Two levels of UV radiation time were 1.0 min and 3.0 min, respectively.

Table 2. Orthogonal experiment of synergistic modification of talcum and calcium carbonate.

Sample	Content of $CaCO_3$ (%)	Content of Talcum (%)	UV Radiation Time (min)	Impact Strength (kg·cm) (Standard Deviation)
1	1.0	1.0	1.0	40 (0.82)
2	1.0	5.0	3.0	50 (1.83)
3	5.0	1.0	3.0	40 (1.63)
4	5.0	5.0	1.0	45 (1.15)

2.3. Characterization

According to GB/T1732-93 [23], the impact strength of coating was measured by the impact force instrument on QCJ impactor (Tianjin Jingkelian Material Testing Machine Co., Ltd., Tianjin, China). In the impact test, the ball falls on the surface of the tested coating (the maximum distance between the ball and the coating is 50 cm, and the weight of the ball is 1 kg). At the end of the test, the deformation on the coating was observed. According to GB/T1720-89 [24], the adhesion of coating was measured by QFZ-II circle-cut coating adhesion tester (Tianjin Jingkelian Material Testing Machine Co., Ltd., Tianjin, China). At the end of the adhesion test, the damage of the coating was observed with a magnifying glass. The top side of the damage on the coatings was marked with 1, 2, 3, 4, 5, 6, and 7 sites, which were called 7 grades. The grade 1 is the strongest adherence, and the grade 7 is the weakest adhesion. If the coating of more than 70% is complete, then it is considered to be good, otherwise it is damaged. According to GB 6739-1996 [25], the hardness of coating was measured. The hardness designation of the pencil that just fails to cut the coating is the hardness of the coating. The hardness of the pencil is as follows: 6H, 5H, 4H, 3H, 2H, 1H, HB, 1B, 2B, 3B, 4B, 5B, and 6B. H means hard, the larger the number of H, the harder it is. B means soft, the bigger the B, the softer it is. The gloss was measured by the BGD512-60° gloss meter (Suzhou Essen Instrument Equipment Co., Ltd., Suzhou, China). The gloss is the percentage of the reflected light of the surface of the coating to the reflected light of the standard plate. According to GB/T1730-2007 GB/T1730-2007 [26], the quality of coating was measured by exposition in 15% NaCl solution. The filter paper, which is soaked in NaCl solution, is placed on the surface of the coating. Then, the coating was covered with a glass cover, and placed for 24 h. The infrared spectroscopy (FT-IR) was performed on the NEXUS-670 spectrometer (Thermo Nicolet Corporation, Madison, SD, USA), and UV analysis was carried out by UV-3600 UV-Vis-NIR spectrophotometer. The micro-morphology of WUVCW was observed by scanning electron microscope (SEM) (SEM, Askashi Seisakusho Ltd., Askashi, Japan) (SX-40). Thermogravimetric analysis (TG-209F3) (NETZSCH Scientific Instruments Ltd., Selb, Germany) was used to determine the thermal stability of the coatings at a heating rate of 10 $^{\circ}C \cdot min^{-1}$ in a nitrogen atmosphere. The orthogonal analysis and interaction were measured by the orthogonal design assistant v3.1 statistical software. The sampling error of the various tests is within 5%. All of the measurements were repeated at least four times, and the reproducibility of the observations was good.

3. Results and Discussion

WUVCW is usually the multilayer coating system, and the layering influenced the performance of coating. Furthermore, the type and quality of substrate influenced the quality of WUVCW [27]. In this paper, the layering and the type and quality of substrate were being considered as constants, and the synergistic effect of talcum and $CaCO_3$ modification on properties of interior waterborne UV-curing coatings on the surface of wood materials was investigated. The three factors of $CaCO_3$, talcum content, and UV irradiation time have a certain effect on mechanical properties (such as adhesion, impact

strength, and hardness) of WUVCW. By comparison, the influence on the impact strength is more obvious. Therefore, in the orthogonal experiment, the analysis was focused on the impact strength of the modified conditions, and then the process parameters were optimized to further explore the effect of modification on other mechanical properties. Table 2 shows the effect of the three factors on impact strength of WUVCW. The main effects plot has been added and showed in Figure 1. The range is the difference between the maximum and the minimum mean value of the same column corresponding to the same factor. The variance of the orthogonal experiment showed the significant effect of the factors on the experimental results. The range and variance between the maximum average impact strength and the minimum average impact strength were displayed in Table 3. The higher range and the greater variance imply the effect of the factor is more significant. Through comparing the range and variance values, the effect of talcum content on the impact strength of WUVCW was most obvious, and the effect of $CaCO_3$ content and UV irradiation time were the minimum. In order to save energy, the UV radiation time was fixed at 1 min in the following experiments. The interactions of talcum and $CaCO_3$ were showed in Table 4. In addition, from Table 2 it is obvious that sample 2 has the good impact strength, that is, the content of $CaCO_3$ is 1.0%, meaning that the independent test $CaCO_3$ content was fixed at 1.0%.

Table 3. Range and variance of synergistic modification of talcum and calcium carbonate.

Factor	Range	Variance
Content of $CaCO_3$ (%)	2.5	6.25
Content of talcum (%)	7.5	56.25
UV radiation time (min)	2.5	6.25

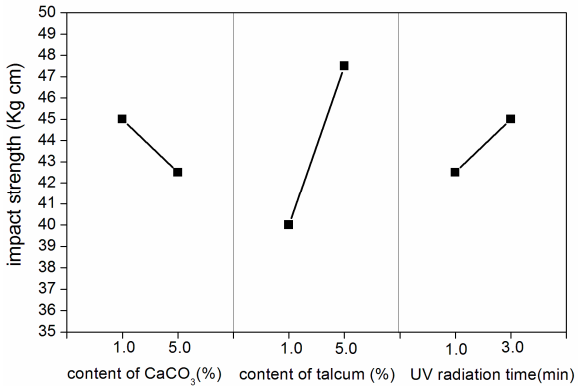

Figure 1. Main effects plot of $CaCO_3$, talcum content and ultraviolet (UV) irradiation time (samples 1–4 in Table 2).

Table 4. Interactions of talcum and $CaCO_3$.

Content of $CaCO_3$ (%)	Content of Talcum (%)	
	1.0	5.0
1.0	40.0	45.0
5.0	40.0	50.0

In order to study the key role of talcum, a series of independent experiments were conducted on the basis of orthogonal experiment. The details of the experiments were the following: the $CaCO_3$ content was fixed at 1.0%, UV irradiation time was 1.0 min, the content of talcum was 0, 1.0%, 2.0%, 3.0%, 4.0%, 5.0%, and 6.0% (samples 1 and 5–10 in Table 1), and the effects of talcum on the mechanical and optical properties of WUVCW were investigated. Table 5 shows the trend of the influence of talcum content on hardness of WUVCW. According to Table 5, the increase of talcum content from 0 to 2.0%

resulted in the increase of the hardness of the coating from 2H to 3H. As shown in thermogravimetric curves (Figure 2) and thermal properties (Table 6), 5% and 10% thermal decomposition temperatures ($T_{5\%}$ and $T_{10\%}$, respectively) of WUVCW with no talcum were 258.48 °C and 280.47 °C, whereas WUVCW with 2.0% talcum content showed highly increased values of 267.43 °C and 291.43 °C, which increased with increasing talcum content. The crosslink would improve stability of polymer, especially for the thermo-stability [28]. It can be seen from the Figure 2 and Table 6 that the temperature of the decomposition increased and the heat resistance with the increased talcum content from 0 to 2.0%, which indicated the crosslink density increase. After adding talcum, the talcum would disperse in WUVCW and crosslink density increased, thus the hardness of the coatings would increase [28]. Continued to increase the talcum content to 4.0%, the hardness of the coating still maintained at 3H. At the same time, the hardness of coatings with talcum content of 2.0%–4.0% was significantly higher than that without talcum. However, when the content of talcum was over 4.0%, the hardness decreased. The agglomeration of particles is easy to occur due to the large amount of talcum (Figure 3). The distribution is uneven or the particle size is too large, which are the stress concentration point, leading to the decrease of hardness. Therefore, the amount of talcum powder should be appropriate to effectively improve the hardness of WUVCW. When the content of talcum is 2.0%–4.0%, the maximum hardness is 3H.

Table 5. Effect of talcum content on properties of the coating during the synergistic effect (samples 1 and 5–10 in Table 1).

Sample	Hardness	Adhesion (Grade)	Impact Strength (kg·cm) (Standard Deviation)	Gloss (%)
5	2H	2	35 (1.47)	64.0
1	2H	1	40 (1.22)	60.0
6	3H	1	40 (0.41)	58.0
7	3H	2	35 (0.81)	50.0
8	3H	2	35 (1.17)	44.0
9	2H	2	35 (0.71)	38.0
10	2H	2	35 (0.81)	32.0

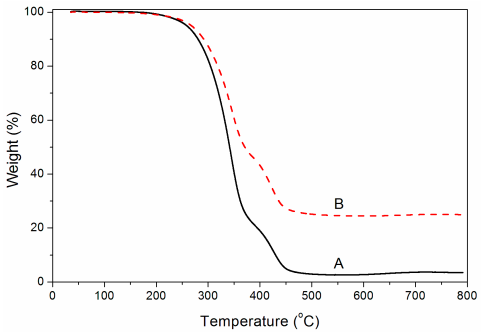

Figure 2. Thermogravimetric curves of WUVCW with 0 (**A**, sample 5) and 2.0% (**B**, sample 6) talcum content.

Table 6. Thermal properties of WUVCW with 0 and 2.0% talcum content.

Sample	Talcum Content (%)	$T_{5\%}$ (°C)	$T_{10\%}$ (°C)
5	0	258.48	280.47
6	2.0	267.43	291.43

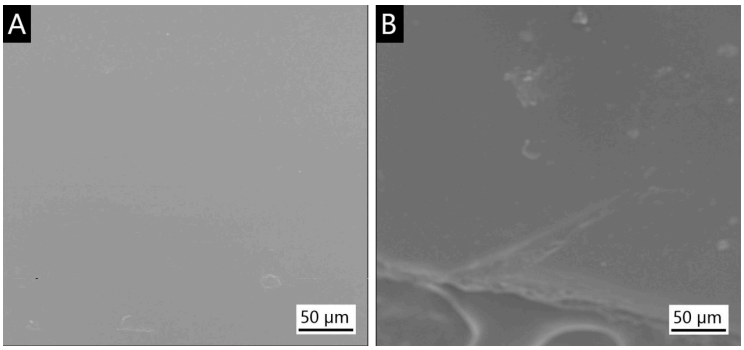

Figure 3. Scanning electron microscope (SEM) of WUVCW from sample 6 and sample 9: (**A**) 1.0% $CaCO_3$ and 2% talcum and (**B**) 1.0% $CaCO_3$ and 5% talcum.

The adhesion of the coating shows the extent to which the coating is attached to the substrate under specified load. The variation of coating adhesion with the content of talcum during the synergistic effect was shown in Table 5. When the content of $CaCO_3$ was fixed at 1.0%, with the increase of the talcum content, the adhesion increased first and then decreased. As can be seen from Table 5, with the talcum content increased from 0 to 1.0%, the adhesion varied greatly from grade 2 to grade 1. When the talcum content continued to increase to 2.0%, the adhesion of the coating maintained at a good level of grade 1. This is due to the cohesion of the coating and mechanical interlocking increase, leading to the increase of adhesion [29]. However, with talcum content increased further from 2.0% to 6.0%, the adhesion declined to grade 2, which was due to the coarse talcum particles, and too much talcum particles will produce aggregation and particles cannot be dispersed evenly. In addition, the increase of talcum powder content makes the elasticity of WUVCW decrease, and reduces the probability of energy consumption under external force [30]. As a result, the WUVCW is easy to break, and the adhesion decreased to grade 2.

Impact resistance is the test of the deformation of the coating at high speed load. The impact resistance of the coating is related to its tensile strength and adhesion. As shown in Table 5, with the fixed content of $CaCO_3$, the increase of talcum content from 0 to 1.0% brought about the increase of impact resistance of WUVCW from 35 kg·cm to 40 kg·cm. As the content of talcum increases to 2.0%, the impact strength of WUVCW was still 40 kg·cm and coating fracture was not observed. However, with the talcum content continuing to increase, the impact resistance of WUVCW decreased. This trend is consistent with the changing trend of adhesion, which shows that the good adhesion of the coating to the dynamic impact test can ensure the better impact resistance of the coating [31].

Influence of talcum content on gloss is shown in Table 5. It showed that when the content of $CaCO_3$ was fixed at 1.0%, the gloss of WUVCW dramatically declined from 64.0% to 32.0% with the increasing of the content of talcum powder from 0 to 6.0%. The talcum powder was insoluble in WUVCW. The talcum was gathered in high content, which can even be seen in surface aggregation phenomenon of WUVCW. With the increasing of the content of talcum, the volume concentration in the surface of the coating is increased, as the talcum powder is insoluble in the WUVCW, and formed the slightly rough surface. When the incident light is irradiated to the rough surface, the light scattering is produced, and the gloss is reduced. According to GB/T3324-2008 [32] wooden furniture general requirements, the value gloss of matte surface is less than 35% [33]. As can be observed from Table 5, WUVCW presented the matte gloss when $CaCO_3$ content was fixed at 1.0% and the content of talcum powder was more than 5.0%.

FT-IR spectra of WUVCW with different $CaCO_3$ and talcum content are illustrated in Figure 4. The assignment of FT-IR band was summarized in Table 7. The band at 3343 cm^{-1} is the wavenumber of N–H stretching vibration. The band at 1724 cm^{-1} can be assigned to be the carbonyl absorption [34]. The characteristic band observed for the N–H bending vibration of amide II band appears at 1530 cm^{-1}, which indicates that the product contains urethane bond. 1670 cm^{-1} is the C=C bond characteristic

absorption band. Band at 2930 cm^{-1} and 1462 cm^{-1} is –CH absorption band. The N–C–O stretching vibration band appears at 1256 cm^{-1}. In addition, the band at 1049 cm^{-1} and 1120 cm^{-1} is also found in Figure 4 corresponding to C–O stretching. After the modification of $CaCO_3$ and talcum, the infrared absorption of WUVCW decreased. After adding the talcum, the absorption band at 1530 cm^{-1} of the FT-IR measurement decreased obviously, which may be the consequence of the reaction of –OH group in talcum ($Mg_3[Si_4O_{10}](OH)_2$) with –NCO [35,36], so that the crosslink density of WUVCW increased and the heat resistance increased (Figure 2).

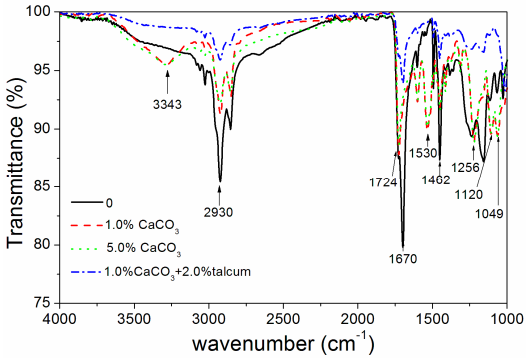

Figure 4. Infrared spectroscopy (FT-IR) of WUVCW with different $CaCO_3$ and talcum content (samples 11, 5, 23 and 6 in Table 1).

Table 7. The assignment of band.

Band (cm^{-1})	Assignment
3343	N–H stretching vibration
1724	carbonyl absorption
1530	N–H bending vibration
1670	C=C bond
2930, 1462	–CH absorption
1049, 1120	C–O stretching
1256	N–C–O stretching vibration

Figure 5 is the UV-Vis spectrum of WUVCW modified by $CaCO_3$ and talcum during the curing process. It was found that the UV light of 200–400 nm was mainly absorbed by the coating and the intensity gradually decreased during the curing process, which indicated that the WUVCW modified by $CaCO_3$ and talcum was cured by absorbing UV light [5].

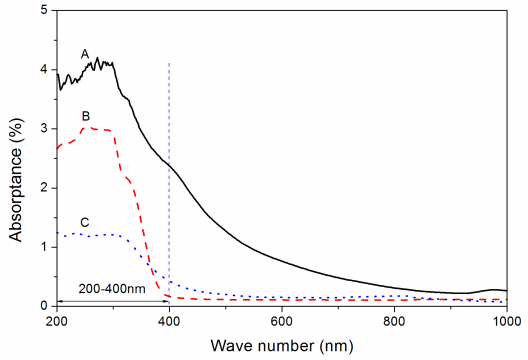

Figure 5. UV-Vis spectrum of WUVCW after adding $CaCO_3$ and talcum (**A**) before curing, (**B**) UV radiation time of 30 s, (**C**) UV radiation time of 1.0 min (sample 6 in Table 1).

The improvement effect of $CaCO_3$ and talcum powder on WUVCW was summarized in Table 8. The mechanical properties of the WUVCW were improved significantly after the $CaCO_3$ and talcum modification, and the gloss was reduced. WUVCW with $CaCO_3$ and talcum modification had better performance than commercial waterborne UV-curing coatings (the last line in Table 8). The surface of talcum has hydrophilic chain, and the hydrophilic chain reacted with –NCO of WUVCW, which increased the crosslink density of WUVCW [36]. The weight change (percentage of residual mass in the quality of the original sample) in the process of coating drying was shown in Figure 6. The weight of WUVCW with talcum powder decreased faster in the early stage of the drying process when compared to WUVCW with no talcum. Therefore, the ability of resistance to external damage of WUVCW was enhanced; in addition, talcum powder can improve the drying speed, so that the mechanical properties of WUVCW were improved. Kaboorani et al. [37] found that the hardness of UV-cured cellulose nanocrystal nanocomposite coating for wood was increased as cellulose nanocrystal loading increased in the coatings, and the hardness was improved from H to 2H by an increase in cellulose nanocrystal loading from 1% to 3%. WUVCW with $CaCO_3$ and talcum modification had been proven to show remarkable property enhancement as compared to other works using additives to UV-curing coatings [15,16,37].

Table 8. Performance comparison of WUVCW with talcum modification.

Sample	Filler Content	Hardness	Adhesion (Grade)	Impact Strength (kg·cm) (Standard Deviation)	Gloss (%)
11	-	H	3	25 (0.82)	88.0
5	1% $CaCO_3$	2H	2	35 (0.81)	64.0
14	2% talcum	2H	2	35 (0.81)	70.0
6	1% $CaCO_3$ + 2% talcum	3H	1	40 (0.41)	58.0
commercial	-	3B	1	10 (0.16)	53.0

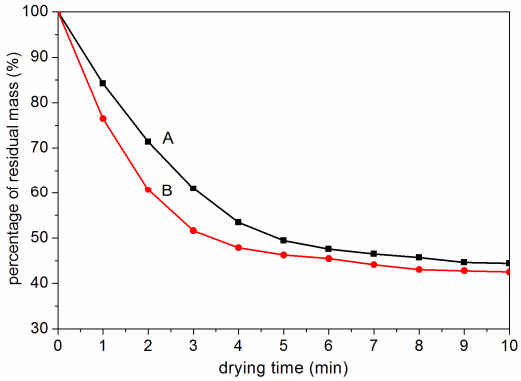

Figure 6. Weight change of WUVCW with the drying time at 40 °C: 0 (**A**, sample 5) and 2.0% (**B**, sample 6) talcum content.

WUVCW with $CaCO_3$ and talcum modification showed excellent resistance against 15% NaCl solution during 24 h exposure, with no appearance change (Table 9), which is a crucial factor for the application of coatings. After the test of resistance against the liquid, the coating can maintain high hardness, adhesion, high impact resistance, and the least gloss loss of the coating.

When the talcum powder was only added in WUVCW (samples 11–18 in Table 1), the hardness, adhesion, impact strength, and gloss change of WUVCW with the content of talcum powder were shown from Figures 7–10. We can notice that the increase of the content of talcum from 0 to 0.5% arouse to increase the hardness of WUVCW from H to 2H, and the adhesion and impact strength were greatly improved to level 2 and 35 kg·cm, respectively. Continued to increase the content of talcum to 2.0%, the hardness of the coating remained 2H, adhesion of coating kept the level 2, and the impact strength was maintained at 35 kg·cm. However, the hardness, adhesion, and impact strength decreased when

the content of talcum was over 2.0%. The gloss of the WUVCW decreases with the increase of the content of talcum. A small increase in the content of talcum powder leads to a large decrease in the gloss of the WUVCW. Moreover, with the increase of content of the talcum powder from 0 to 6.0%, the gloss of the WUVCW continued to slow down from 88% to 32%. That is, when the content of talcum powder was 2.0%, the WUVCW exhibited a lower gloss and better mechanical property.

Table 9. Solvent resistance of WUVCW after exposition of 15% NaCl solution.

Sample	Filler Content	Hardness	Adhesion (grade)	Impact Strength (kg·cm) (Standard Deviation)	Gloss (%)	Gloss Change (%)
11	-	B	4	20 (1.15)	84.5	3.5
5	1% $CaCO_3$	2H	2	35 (0.82)	59.0	5.0
14	2% talcum	2H	2	35 (0.82)	68.0	2.0
6	1% $CaCO_3$ + 2% talcum	3H	1	40 (1.63)	57.0	1.0
commercial	-	5B	3	5 (0.16)	47.0	6.0

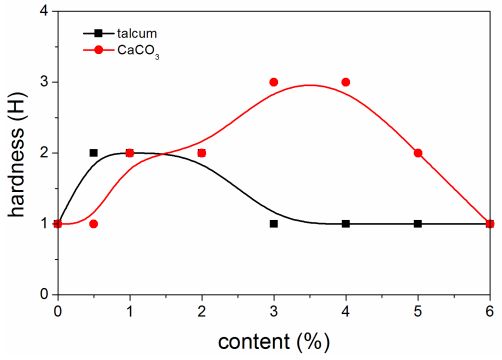

Figure 7. Effect of single filler on hardness of coating (samples 5, 11–24 in Table 1).

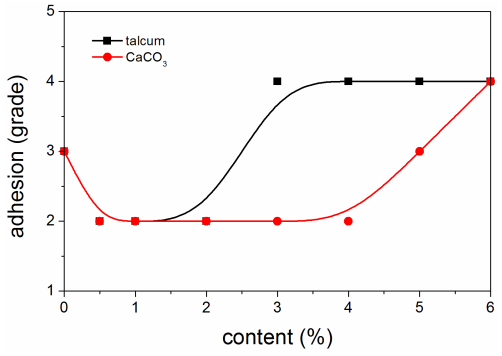

Figure 8. Effect of single filler on adhesion of coating (samples 5, 11–24 in Table 1).

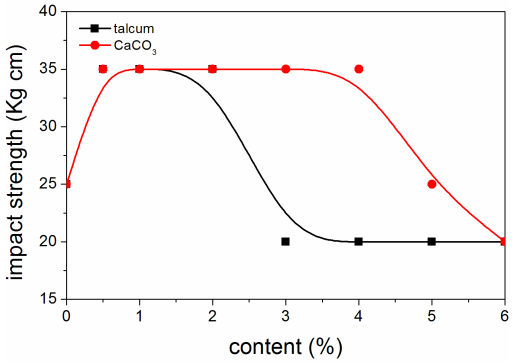

Figure 9. Effect of single filler on impact strength of coating (samples 5, 11–24 in Table 1).

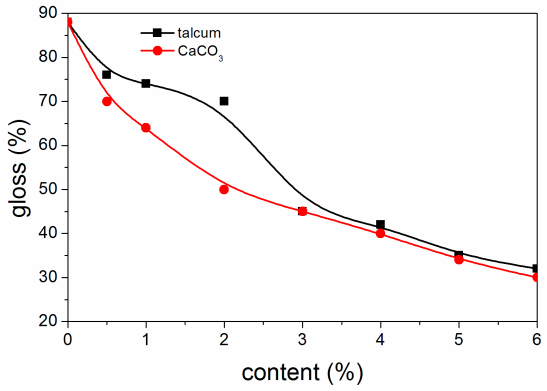

Figure 10. Effect of single filler on gloss of coating (samples 5, 11–24 in Table 1).

Effects of single filler $CaCO_3$ (samples 5, 19–24 in Table 1) on mechanical properties of WUVCW showed that when the $CaCO_3$ content was 3.0%–4.0%, WUVCW had good hardness, adhesion, and impact strength, which were 3H, grade 2, and 35 kg·cm, respectively. However, when the $CaCO_3$ content was higher than 4.0%, the hardness, adhesion, and impact resistance decreased. The gloss results showed that gloss of WUVCW decreases with the $CaCO_3$ content. When $CaCO_3$ content was 3.0%–4.0%, the obtained WUVCW showed better mechanical properties and matte gloss.

4. Conclusions

In this study, synergistic effect of talcum and $CaCO_3$ modification on properties of interior WUVCW was optimized by the orthogonal experiment. When the content of $CaCO_3$ was 1.0%, the radiation time of UV lamp was 1.0 min, and the content of talcum powder was 2.0%, the WUVCW had 3H hardness, 40 kg·cm impact strength, and grade-1 adhesion, respectively. With the content of talcum powder increased from 0 to 6.0%, the gloss of WUVCW decreased. When the content of talcum powder was higher than 5.0%, the coating has the matte gloss. When compared with the existence of single filler $CaCO_3$ or talcum powder, WUVCW had better performance when $CaCO_3$ and talcum powder were present at the same time. After the synergistic effect of talcum and $CaCO_3$ modification, the addition of small amount of filler could make the mechanical properties of WUVCW improve and the gloss decrease obviously. It provides a good prospect for the application of waterborne UV-curing coatings on the wood surface.

Acknowledgments: This project is supported by the Natural Science Foundation of Jiangsu Province (BK20150887), Youth Science and Technology Innovation Fund of Nanjing Forestry University (CX2016018) and Priority Academic Program Development of Jiangsu Higher Education Institutions (PAPD).

Author Contributions: Xiaoxing Yan and Xingyu Qian conceived and performed the experiments; Xiaoxing Yan and Rong Lu analyzed the data and wrote the paper; Tetsuo Miyakoshi contributed the analysis tools and checked the English.

Conflicts of Interest: The author declares there are no potential conflicts interests.

References

1. Guo, H.Z.; Fuchs, P.; Cabane, E.; Michen, B.; Hagendorfer, H.; Romanyuk, Y.E.; Burgert, I. UV-protection of wood surfaces by controlled morphology fine-tuning of ZnO nanostructures. *Holzforschung* **2016**, *70*, 699–708. [CrossRef]
2. Wu, J.B.; Zhang, R.F.; Ma, G.Z.; Hou, C.Y.; Zhang, H. Preparation and properties of fluorinated oligomer with tertiary amine structure in the UV curable coatings. *J. Appl. Polym. Sci.* **2017**, *134*. [CrossRef]
3. Zhang, S.W.; Yu, A.X.; Song, X.Q.; Liu, X.Y. Synthesis and characterization of waterborne UV-curable polyurethane nanocomposites based on the macromonomer surface modification of colloidal silica. *Prog. Org. Coat.* **2013**, *76*, 1032–1039. [CrossRef]

4. Yan, X.X.; Xu, G.Y. Influence of silane coupling agent on corrosion-resistant property in low infrared emissivity Cu/polyurethane coating. *Prog. Org. Coat.* **2012**, *73*, 232–238. [CrossRef]
5. Herrera, R.; Muszynska, M.; Krystofiak, T.; Labidi, J. Comparative evaluation of different thermally modified wood samples finishing with UV-curable and waterborne coatings. *Appl. Surf. Sci.* **2015**, *357*, 1444–1453. [CrossRef]
6. Wan, T.; Chen, D.J. Synthesis and properties of self-healing waterborne polyurethanes containing disulfide bonds in the main chain. *J. Mater. Sci.* **2017**, *52*, 197–207. [CrossRef]
7. Du, W.N.; Liu, J.; Wang, Y.F.; Li, Y.P.; Li, Z.J. Polyurethane encapsulated carbon black particles and enhanced properties of water polyurethane composite films. *Prog. Org. Coat.* **2016**, *97*, 146–152. [CrossRef]
8. Zhang, S.W.; Chen, Z.D.; Guo, M.; Bai, H.Y.; Liu, X.Y. Synthesis and characterization of waterborne UV-curablepolyurethane modified with side-chain triethoxysilaneand colloidal silica. *Colloids Surf. A Physicochem. Eng. Asp.* **2015**, *468*, 1–9. [CrossRef]
9. Liu, H.J.; Li, C.; Sun, X.S. Soy-oil-based waterborne polyurethane improved wet strength of soy protein adhesives on wood. *Int. J. Adhes. Adhes.* **2017**, *73*, 66–74. [CrossRef]
10. Llorente, O.; Fernandez-Berridi, M.J.; Gonzalez, A.; Irusta, L. Study of the crosslinking process of waterborne UV curable polyurethane acrylates. *Prog. Org. Coat.* **2016**, *99*, 437–442. [CrossRef]
11. Krystofiak, T.; Lis, B.; Muszynska, M.; Proszyk, S. The effect of aging tests on gloss and adhesion of lacquer coatings on window elements from pine wood. *Drewno* **2016**, *59*, 127–137.
12. Lu, Z.G.; Tang, T.; Zhou, G.; Jia, W.D.; Wang, M.; Xu, J.; Bai, S.H. Effect of dehumidification drying environment on surface gloss of one component waterborne wood top coating. *Appl. Therm. Eng.* **2016**, *102*, 716–719. [CrossRef]
13. Baba, B.O. Curved sandwich composites with layer-wise graded cores under impact loads. *Compos. Struct.* **2017**, *159*, 1–11. [CrossRef]
14. Scrinzi, E.; Rossi, S.; Deflorian, F.; Zanella, C. Evaluation of aesthetic durability of waterborne polyurethane coatings applied on wood for interior applications. *Prog. Org. Coat.* **2011**, *72*, 81–87. [CrossRef]
15. Wu, K.H.; Xiang, S.L.; Zhi, W.Q.; Bian, R.J.; Wang, C.C.; Cai, D.Y. Preparation and characterization of UV curable waterborne poly(urethane-acrylate)/antimony doped tin oxide thermal insulation coatings by sol-gel process. *Prog. Org. Coat.* **2017**, *113*, 39–46. [CrossRef]
16. Liao, H.Z.; Zhang, B.; Huang, L.H.; Ma, D.; Jiao, Z.P.; Xie, Y.S.; Tan, S.Z.; Cai, X. The utilization of carbon nitride to reinforce the mechanical and thermal properties of UV-curable waterborne polyurethane acrylate coatings. *Prog. Org. Coat.* **2015**, *89*, 35–41. [CrossRef]
17. Rahman, O.; Kashif, M.; Ahmad, S. Nanoferrite dispersed waterborne epoxy-acrylate: Anticorrosive Nanocomposite coatings. *Prog. Org. Coat.* **2015**, *80*, 77–86. [CrossRef]
18. Lv, C.H.; Hu, L.; Yang, Y.; Li, H.B.; Huang, C.; Liu, X.H. Waterborne UV-curable polyurethane acrylate/silica nanocomposites for thermochromic coatings. *RSC Adv.* **2015**, *5*, 25730–25737. [CrossRef]
19. Liu, Z.; Wang, W.W.; Chen, H.; Liu, J.P.; Zhang, W.L. Novel application method of talcum powder to prevent sticking tendency and modify release of esomeprazole magnesium enteric-coated pellets. *Pharm. Dev. Technol.* **2016**, *21*, 405–414. [CrossRef] [PubMed]
20. Wang, L.; Ling, X.L.; Guo, Z.X.; Yu, J. Effects of talcum powder (talc) and compounding sequence on the morphology and mechanical properties of PA6/PP/MAPP blend. *Chem. J. Chin. Univ.* **2012**, *33*, 2789–2794.
21. Panda, B.; Digdarsini, T.; Mallick, S. Physicomechanical and physicochemical characterizations of biexponential compaction process of paracetamol in the presence of talcum-lubricated-MCC. *Powder Technol.* **2015**, *273*, 91–101. [CrossRef]
22. Kuusisto, J.; Tiittanen, B.T.; Maloney, T.C. Property optimization of calcium carbonate precipitated in a high shear, circulation reactor. *Powder Technol.* **2016**, *303*, 241–250. [CrossRef]
23. *GB/T 1732-93 Determination of Impact Resistance of Film*; Standardization Administration of the Peoples's Republic of China: Beijing, China, 1993; pp. 418–420. (In Chinese)
24. *GB/T 1720-89 Determination of Adhesion of Film*; Standardization Administration of the Peoples's Republic of China: Beijing, China, 1979; pp. 378–379. (In Chinese)
25. *GB 6739-1996 Determination of Film Hardness by Pencil Test*; Standardization Administration of the Peoples's Republic of China: Beijing, China, 1996; pp. 1–4. (In Chinese)
26. *GB/T1730-2007 Paints and Varnishes-Pendulum Damping Test*; Standardization Administration of the Peoples's Republic of China: Beijing, China, 2007; pp. 1–11. (In Chinese)

27. Martin, D.; Martin, T.; Vladimir, B.; Tomas, R.; Lenka, K.; Peter, K. Influence of substrate material and its plasma pretreatment on adhesion and properties of WC/a-C:H nanocomposite coatings deposited at low temperature. *Surf. Coat. Technol.* **2018**, *333*, 138–147.
28. Pittayavinai, P.; Thanawan, S.; Amornsakchai, T. Manipulation of mechanical properties of short pineapple leaf fiber reinforced natural rubber composites through variations in cross-link density and carbon black loading. *Polym. Test.* **2016**, *54*, 84–89. [CrossRef]
29. Matsuzaki, R.; Tsukamoto, N.; Taniguchi, J. Mechanical interlocking by imprinting of undercut micropatterns for improving adhesive strength of polypropylene. *Int. J. Adhes. Adhes.* **2016**, *68*, 124–132. [CrossRef]
30. Jung, J.; Deng, Z.L.; Simonsen, J.; Bastias, R.M.; Zhao, Y.Y. Development and preliminary field validation of water-resistant cellulose nanofiber based coatings with high surface adhesion and elasticity for reducing cherry rain-cracking. *Sci. Hortic.* **2016**, *200*, 161–169. [CrossRef]
31. Shi, X.Y.; Lian, C.B.; Shang, Y.Y.; Zhang, H.Y. Evolution of the dynamic fatigue failure of the adhesion between rubber and polymer cords. *Polym. Test.* **2015**, *48*, 175–182. [CrossRef]
32. *GB/T3324-2008 Wooden Furniture-General Technical Requirements*; Standardization Administration of the Peoples's Republic of China: Beijing, China, 2008; pp. 1–16. (In Chinese)
33. Toscani, M.; Valsecchi, M.; Gegenfurtner, K.R. Lightness perception for matte and glossy complex shapes. *Vis. Res.* **2017**, *131*, 82–95. [CrossRef] [PubMed]
34. Xu, H.P.; Qiu, F.X.; Wang, Y.Y.; Wu, W.L.; Yang, D.Y.; Guo, Q. UV-curable waterborne polyurethane-acrylate: Preparation, characterization and properties. *Prog. Org. Coat.* **2012**, *73*, 47–53. [CrossRef]
35. Lin, W.T.; Lee, W.J. Effects of the NCO/OH molar ratio and the silica contained on the properties of waterborne polyurethane resins. *Colloid Surf. A.* **2017**, *522*, 453–460. [CrossRef]
36. Katiyar, J.K.; Sinha, S.K.; Kumar, A. Friction and wear durability study of epoxy-based polymer (SU-8) composite coatings with talc and graphite as fillers. *Wear* **2016**, *362*, 199–208. [CrossRef]
37. Kaboorani, A.; Auclair, N.; Riedl, B.; Landry, V. Mechanical properties of UV-cured cellulose nanocrystal (CNC) nanocomposite coating for wood furniture. *Prog. Org. Coat.* **2017**, *104*, 91–96. [CrossRef]